

Pyrazolato-Bridged Polynuclear Palladium and Platinum Complexes. Synthesis, Structure, and Reactivity

Keisuke Umakoshi,^{*,†} Yoko Yamauchi,[†] Keiko Nakamiya,[†] Takashi Kojima,[†] Mikio Yamasaki,[‡] Hiroyuki Kawano,^{†,§} and Masayoshi Onishi^{*,†}

Department of Applied Chemistry, Faculty of Engineering, Nagasaki University, Bunkyo-machi, Nagasaki 852-8521, Japan, and Rigaku Corporation, Matsubara, Akishima, Tokyo 196-8666, Japan

Received November 20, 2002

Cyclic trinuclear complexes [Pd₃(μ-pz)₆] (1) and [Pd₃(μ-4-Mepz)₆] (2) and dinuclear complex [Pd₂(μ-3-*t*-Bupz)₂(3-*t*-Bupz)₂(3-*t*-BupzH)₂] (3) have been prepared by the reactions of [PdCl₂(CH₃CN)₂] with pyrazole (pzH), 4-methylpyrazole (4-MepzH), and 3-*tert*-butylpyrazole (3-*t*-BupzH), respectively, in CH₃CN in the presence of Et₃N. In the absence of the base, treatment of [PdCl₂(CH₃CN)₂] with pzH gave the mononuclear complex, [Pd(pzH)₄]Cl₂ (6). The reaction of [PtCl₂(C₂H₅CN)₂] with pzH in the presence of Et₃N under refluxing in C₂H₅CN afforded the known dimeric Pt(II) complex, [Pt(pz)₂(pzH)₂] (7). The protons participating in the hydrogen bonding in 3 and 7 are easily replaced by silver ions to give the heterotetranuclear complex [Pd₂Ag₂(μ-3-*t*-Bupz)₄] (4) and the heterohexanuclear complex [Pt₂Ag₄(μ-pz)₈] (5). The complexes 1–6 are structurally characterized.

Introduction

Polynuclear transition metal complexes with pyrazoles and/or pyrazolates have been attracting attention because of their versatile structures and properties.^{1–5} The reaction conditions and the nature of the central metal ions take part in whether coordinated pyrazoles exist as the protonated form (pyrazoles) or the deprotonated form (pyrazolates). The protons in coordinated pyrazoles often participate in the intra- or intermolecular hydrogen bonding.⁴ Pyrazolates usually^{6,7} act as bridging ligands, though the number of reports relating to homoleptic pyrazolato (η²-pyrazolato) complexes is gradually increasing.^{6–13} By using the bridging ability of pyrazolates, it is possible to construct cyclic polynuclear

complexes. Although tetranuclear,^{14–16} hexanuclear,¹⁷ or octanuclear¹⁸ cyclic complexes are also known, the most popular cyclic complex is the trinuclear one, in which monovalent two-coordinate metal ions are singly bridged by pyrazolates to form [M¹₃(μ-Rpz)₃] (M = Ag,^{17,19–21} Au,^{17,22–26}

* To whom correspondence should be addressed. E-mail: kumks@net.nagasaki-u.ac.jp (K.U.); onishi@net.nagasaki-u.ac.jp (M.O.).

[†] Nagasaki University.

[‡] Rigaku Corporation.

[§] Present address: General Education Department, Kogakuin University, Hachioji, Tokyo 192-0015, Japan.

(1) Trofimenko, S. *Chem. Rev.* **1972**, *72*, 497.

(2) Trofimenko, S. *Prog. Inorg. Chem.* **1986**, *34*, 115.

(3) Sadimenko, A. P.; Basson, S. S. *Coord. Chem. Rev.* **1996**, *147*, 247.

(4) La Monica, G.; Ardizzoia, G. A. *Prog. Inorg. Chem.* **1997**, *46*, 151.

(5) Sadimenko, A. P. *Adv. Heterocycl. Chem.* **2001**, *80*, 157.

(6) Deacon, G. B.; Delbridge, E. E.; Skelton, B. W.; White, A. H. *Angew. Chem., Int. Ed.* **1998**, *37*, 2251.

(7) Guzei, I. A.; Yap, G. P. A.; Winter, C. H. *Inorg. Chem.* **1997**, *36*, 1738.

(8) Gust, K. R.; Knox, J. E.; Heeg, M. J.; Schlegel, H. B.; Winter, C. H. *Angew. Chem., Int. Ed.* **2002**, *41*, 1591.

(9) Most, K.; Köpke, S.; Dall'Antonia, F.; Mösch-Zanetti, N. C. *Chem. Commun.* **2002**, 1676.

(10) Mösch-Zanetti, N. C.; Krätzner, R.; Lehmann, C.; Schneider, T. R.; Usón, I. *Eur. J. Inorg. Chem.* **2000**, 13.

(11) Pfeiffer, D.; Ximba, B. J.; Liable-Sands, L. M.; Rheingold, A. L.; Heeg, M. J.; Coleman, D. M.; Schlegel, H. B.; Kuech, T. F.; Winter, C. H. *Inorg. Chem.* **1999**, *38*, 4539.

(12) Cosgriff, J. E.; Deacon, G. B. *Angew. Chem., Int. Ed.* **1998**, *37*, 286.

(13) Pfeiffer, D.; Heeg, M. J.; Winter, C. H. *Angew. Chem., Int. Ed.* **1998**, *37*, 2517.

(14) Ardizzoia, G. A.; Cenini, S.; La Monica, G.; Masciocchi, N.; Moret, M. *Inorg. Chem.* **1994**, *33*, 1458.

(15) Zhang, H.; Fu, D.; Ji, F.; Wang, G.; Yu, K.; Yao, T. *J. Chem. Soc., Dalton Trans.* **1996**, 3799.

(16) Ardizzoia, G. A.; Cenini, S.; La Monica, G.; Masciocchi, N.; Maspero, A.; Moret, M. *Inorg. Chem.* **1998**, *37*, 4284.

(17) Murray, H. H.; Raptis, R. G.; Fackler, J. P., Jr. *Inorg. Chem.* **1988**, *27*, 26.

(18) Ardizzoia, G. A.; Angaroni, M. A.; La Monica, G.; Cariati, F.; Cenini, S.; Moret, M.; Masciocchi, N. *Inorg. Chem.* **1991**, *30*, 4347.

(19) Masciocchi, N.; Moret, M.; Cairati, P.; Sironi, A.; Ardizzoia, G. A.; La Monica, G. *J. Am. Chem. Soc.* **1994**, *116*, 7668.

(20) Meyer, F.; Jacobi, A.; Zsolnai, L. *Chem. Ber.* **1997**, *130*, 1441.

(21) Dias, H. V. R.; Polach, S. A.; Wang, Z. *J. Fluorine Chem.* **2000**, *103*, 163.

(22) Bovio, B.; Bonati, F.; Banditelli, G. *Inorg. Chim. Acta* **1984**, *87*, 25.

(23) Raptis, R. G.; Murray, H. H.; Fackler, J. P., Jr. *Acta Crystallogr.* **1988**, *C44*, 970.

(24) Raptis, R. G.; Fackler, J. P., Jr. *Inorg. Chem.* **1990**, *29*, 5003.

Co,²⁷ Cu,^{16,19,21,28–32} Rpz = pyrazolate or substituted pyrazolates). Until very recently, the only exception of the pyrazolate-bridged cyclic trinuclear complex having a different metal/ligand ratio was [Pt₃(μ-pz)₆], which was prepared by the specific method in a sealed tube.³³ The cyclic trinuclear palladium(II) complex with 3-phenylpyrazolate has just been prepared by the stepwise manner by Raptis and co-workers.³⁴

We have recently reported the variable-temperature ¹H NMR spectra of [Pd(η³-2-methylallyl){B(3-*t*-Bupz)₄}] (3-*t*-Bupz = 3-*tert*-butylpyrazol-1-yl group)³⁵ and discussed the stereochemical nonrigidity in the square-planar Pd(II) complex of the tetrakis(pyrazol-1-yl)borate ligand containing a bulky 3-substituent.³⁶ In order to further elucidate the correlation of the nonrigid motions of the B(3-*t*-Bupz)₄ ligand with a trans-coexisting ligand, we tried to prepare the Pd(II) complex of B(3-*t*-Bupz)₄ with bulky tropolonate. In spite of our efforts, it was unsuccessful. However, in the reaction of unisolated [PdCl(tropolonato)(CH₃CN)] with K[B(3-*t*-Bupz)₄] in the presence of Ag⁺ ion, we unexpectedly obtained a mixed-metal complex, [Pd₂Ag₂(μ-3-*t*-Bupz)₆], which was formed by the B–N bond cleavage of B(3-*t*-Bupz)₄ ligand. This finding prompted us to undertake a systematic investigation on the Pd(II)–pyrazolate system and led us to the isolation of pyrazolate-bridged cyclic trinuclear Pd(II) complexes, [Pd₃(μ-pz)₆] and [Pd₃(μ-4-Mepz)₆]. The structures of cyclic trinuclear complexes with pyrazolates are very similar to that of palladium acetate [Pd₃(μ-OAc)₆].^{37–39} Thus it is worth comparing the structures and properties of the complexes having nonsubstituted pyrazolate and acetate ligands.

In this paper, we report the synthesis and structural characterization of pyrazolate-bridged cyclic trinuclear Pd(II) complexes, a dinuclear Pd(II) complex, and heteropolynuclear Pd(II) and Pt(II) complexes. The easy replacement of protons in the neutral complexes by Ag⁺ ions is also reported.

Experimental Section

Materials. [PdCl₂(CH₃CN)₂],⁴⁰ [PtCl₂(C₂H₅CN)₂],⁴¹ [PtCl₂(pzH)₂],⁴² 3-*tert*-butylpyrazole (3-*t*-BupzH),³⁵ and potassium tetrakis(3-*tert*-butylpyrazol-1-yl)borate (K{B(3-*t*-Bupz)₄})³⁵ were prepared by the literature methods. Acetonitrile was dried over calcium hydride and distilled under an argon atmosphere. All other commercially available reagents were used as purchased.

Preparation of Complexes. [Pd₃(μ-pz)₆] (1). Method A. An acetonitrile solution (100 mL) containing [PdCl₂(CH₃CN)₂] (137 mg, 0.53 mmol), pyrazole (pzH; 108 mg, 1.59 mmol), and triethylamine (Et₃N; 160 mg, 1.58 mmol) was stirred for 30 min at 25 °C. A white solid of polymeric species ([Pd(Rpz)₂]_n, in Scheme 1) was then filtered off. The filtrate was concentrated slowly under air. The pale yellow crystals were collected, washed with acetonitrile, and dried in air. Yield: 28 mg (22%). The yield depends on the reaction conditions, especially on the amount of solvent employed. The relationship between yield and the concentration of [PdCl₂(CH₃CN)₂] in acetonitrile is summarized in Scheme 1. Anal. Calcd for C₂₂H₂₄N₁₄Pd₃ ([Pd₃(pz)₆]·2CH₃CN): C, 32.87; H, 3.01; N, 24.40. Found: C, 32.89; H, 3.31; N, 24.52. ¹H NMR (CDCl₃)/ppm: δ 5.97 (t, 1H, H₄), 7.35 (d, 2H, H₃ and H₅). FABMS: *m/z* 722 ([M]⁺). Although fresh crystals include acetonitrile molecules as solvent of crystallization, the crystals have low solubility toward acetonitrile. However, **1** can be recrystallized from chloroform and dichloromethane. The recrystallization of **1** from CH₂Cl₂/MeOH in the presence of LiClO₄ gave crystals, which do not include any solvent of crystallization.

Method B. To an acetonitrile solution (100 mL) of [Pd(pzH)₄]Cl₂ (**3**) (181 mg, 0.40 mmol) was added Et₃N (191 mg, 1.9 mmol), and the solution was stirred for 1 h at 20 °C. After removal of a white solid of polymeric species, the filtrate was slowly concentrated under air. The pale yellow crystals were collected, washed with acetonitrile, and dried in air. Yield: 33 mg (34%).

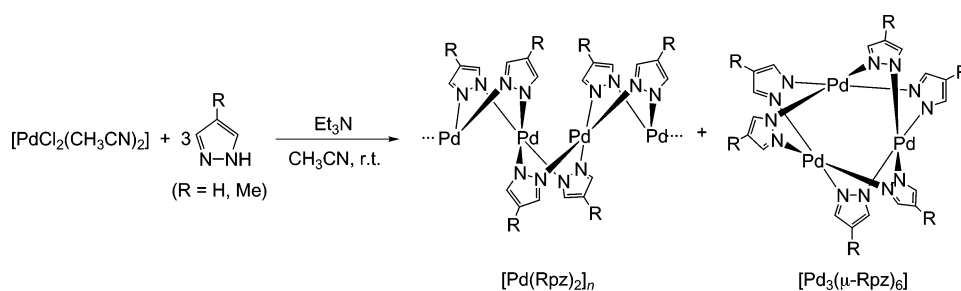
[Pd₃(μ-4-Mepz)₆] (2). To an acetonitrile solution (100 mL) of [PdCl₂(CH₃CN)₂] (131 mg, 0.51 mmol) were added 4-methylpyrazole (4-MepzH; 127 mg, 1.55 mmol) and Et₃N (152 mg, 1.50 mmol), and the solution was stirred for 30 min at 25 °C. After removal of a white solid of polymer, the filtrate was slowly concentrated under air. The pale yellow crystals were collected, washed with acetonitrile, and dried in air. Yield: 22 mg (16%). Anal. Calcd for C₂₄H₃₀N₁₂Pd₃: C, 35.77; H, 3.75; N, 20.86. Found: C, 35.93; H, 3.77; N, 20.80. ¹H NMR (CDCl₃)/ppm: δ 1.89 (s, 3H, Me), 7.09 (s, 2H, H₃ and H₅). FABMS: *m/z* 806 ([M]⁺).

[Pd₂(μ-3-*t*-Bupz)₂(3-*t*-Bupz)₂(3-*t*-BupzH)₂] (3). Method A. To an acetonitrile solution (100 mL) of [PdCl₂(CH₃CN)₂] (131 mg, 0.51 mmol) were added 3-*tert*-butylpyrazole (3-*t*-BupzH; 187 mg, 1.51 mmol) and Et₃N (152 mg, 1.50 mmol), and the solution was stirred for 1 h at 25 °C. No white solid of polymer appeared. The solution was filtered and concentrated under air. The pale yellow crystals were collected before the precipitation of Et₃NHCl, washed with acetonitrile, and dried in air. Yield: 33 mg (14%). The preparation in the presence of Proton Sponge (1,8-bis(*N,N*-dimethylamino)naphthalene) instead of Et₃N also afforded **3** in 29% yield. Anal. Calcd for C₄₂H₆₈N₁₂Pd₂: C, 52.88; H, 7.19; N, 17.62. Found: C, 52.85; H, 7.09; N, 17.64. ¹H NMR (C₆D₆)/ppm: δ 1.26 (s, 18H, *t*-Bu), 1.35 (s, 18H, *t*-Bu), 1.41 (s, 18H, *t*-Bu), 5.89 (d,

- (25) Kim, S. J.; Kang, S. H.; Park, K.-M.; Kim, H.; Zin, W.-C.; Choi, M.-G.; Kim, K. *Chem. Mater.* **1998**, *10*, 1889.
 (26) Barberá, J.; Elduque, A.; Giménez, R.; Lahoz, F. J.; López, J. A.; Oro, L. A.; Serrano, J. L. *Inorg. Chem.* **1998**, *37*, 2960.
 (27) Lukaszewicz, M.; Ciunik, Z.; Mazurek, J.; Sobczak, J.; Staron, A.; Wolowicz, S.; Ziolkowski, J. J. *Eur. J. Inorg. Chem.* **2001**, 1575.
 (28) Raptis, R. G.; Fackler, J. P., Jr. *Inorg. Chem.* **1988**, *27*, 4179.
 (29) Ehlert, M. K.; Rettig, S. J.; Storr, A.; Thompson, R. C.; Trotter, J. *Can. J. Chem.* **1990**, *68*, 1444.
 (30) Ehlert, M. K.; Rettig, S. J.; Storr, A.; Thompson, R. C.; Trotter, J. *Can. J. Chem.* **1992**, *70*, 2161.
 (31) Ehlert, M. K.; Storr, A.; Summers, D. A.; Thompson, R. C. *Can. J. Chem.* **1997**, *75*, 491.
 (32) Angaridis, P. A.; Baran, P.; Boca, R.; Cervantes-Lee, F.; Haase, W.; Mezei, G.; Raptis, R. G.; Werner, R. *Inorg. Chem.* **2002**, *41*, 2219.
 (33) Burger, W.; Strähle, J. Z. *Anorg. Allg. Chem.* **1985**, 529, 111.
 (34) Baran, P.; Marrero, C. M.; Pérez, S.; Raptis, R. G. *Chem. Commun.* **2002**, 1012.
 (35) Trofimenko, S.; Calabrese, J. C.; Thompson, J. S. *Inorg. Chem.* **1987**, *26*, 1507.
 (36) Onishi, M.; Yamaguchi, M.; Nishimoto, E.; Itoh, Y.; Nagaoka, J.; Umakoshi, K.; Kawano, H. *Inorg. Chim. Acta* **2003**, *343*, 111.
 (37) Skapski, A. C.; Smart, M. L. *Chem. Commun.* **1970**, 658.
 (38) Lyalina, N. N.; Dargina, S. V.; Sobolev, A. N.; Buslaeva, T. M.; Romm, I. P. *Koord. Khim.* **1993**, *19*, 57.
 (39) Cotton, F. A.; Han, S. *Rev. Chim. Miner.* **1983**, *20*, 496.

- (40) Wimmer, F. L.; Wimmer, S.; Castan, P.; Puddephatt, R. J. *Inorg. Synth.* **1992**, *29*, 185.
 (41) Kukushkin, V. Yu.; Oskarsson, Å.; Elding, L. I.; Jonasdottir, S. *Inorg. Synth.* **1997**, *31*, 279.
 (42) van Kralingen, C. G.; de Ridder, J. K.; Reedijk, J. *Transition Met. Chem.* **1980**, *5*, 73.

Scheme 1



Concentration Dependence of the Yield ([PdCl ₂ (CH ₃ CN) ₂] = 0.5 mmol)	Yield	Volume
	[Pd ₃ (μ-pz) ₆]	9 %
22		100
30		200
[Pd ₃ (μ-4-Mepz) ₆]	16	100

2H, H₄), 5.95 (d, 2H, H₄), 5.98 (d, 2H, H₄), 6.77 (d, 2H, H₅), 7.31 (d, 2H, H₅), 7.62 (d, 2H, H₅). FABMS: *m/z* 955 ([M + H]⁺).

Method B. An acetonitrile solution (30 mL) containing [PdCl₂(CH₃CN)₂] (51 mg, 0.19 mmol) and sodium tropolonate (60 mg, 0.42 mmol) was stirred for 20 min at 20 °C and filtered. To the filtrate was added K{B(3-*t*-Bupz)₄} (103 mg, 0.19 mmol), and the solution was stirred for 30 min at 20 °C. The solution was filtered and concentrated under air. The pale yellow crystals were collected, washed with acetonitrile, and dried in air. Yield: 20 mg (21%).

[Pd₂Ag₂(μ-3-*t*-Bupz)₆] (4). **Method A.** To an acetonitrile solution (90 mL) of [PdCl₂(CH₃CN)₂] (132 mg, 0.51 mmol) was added an acetonitrile solution (10 mL) of AgPF₆ (380 mg, 1.50 mmol). The solution was stirred for 30 min at 25 °C, and the resulting AgCl was filtered off. An acetonitrile solution (50 mL) of 3-*t*-BupzH (190 mg, 1.53 mmol) and Et₃N (156 mg, 1.54 mmol) was added to the filtrate, and the solution was stirred for 40 min at 25 °C. After filtration, the filtrate was concentrated under air. The colorless crystals were collected, washed with acetonitrile, and dried in air. Yield: 51 mg (17%). Anal. Calcd for C₄₂H₆₆Ag₂N₁₂Pd₂: C, 43.20; H, 5.70; N, 14.39. Found: C, 43.17; H, 5.92; N, 14.56. ¹H NMR (CDCl₃)/ppm: δ 1.20 (s, 18H, *t*-Bu), 1.30 (s, 18H, *t*-Bu), 1.32 (s, 18H, *t*-Bu), 5.77 (d, 2H, H₄), 6.02 (m, 2H, H₄), 6.17 (m, 2H, H₄), 6.48 (d, 2H, H₅), 7.71 (t, 2H, H₅), 7.83 (t, 2H, H₅).

Method B. To an acetonitrile suspension (50 mL) of **3** (139 mg, 0.15 mmol) were added Et₃N (94 mg, 0.93 mmol) and an acetonitrile solution (5 mL) of AgPF₆ (79 mg, 0.31 mmol). The suspension was stirred for 30 min at 25 °C to give a clear solution. After filtration, the filtrate was concentrated under air. The crystals were collected, washed with acetonitrile, and dried in air. Yield: 101 mg (59%).

Method C. An acetonitrile solution (60 mL) containing [PdCl₂(CH₃CN)₂] (234 mg, 0.90 mmol), sodium tropolonate (285 mg, 1.98 mmol), and AgPF₆ (228 mg, 0.90 mmol) was stirred for 1 h at 20 °C and filtered to remove AgCl and NaCl. To the filtrate were added AgPF₆ (228 mg, 0.90 mmol) and K{B(3-*t*-Bupz)₄} (487 mg, 0.90 mmol), and the solution was stirred for 30 min at 20 °C. The solution was filtered and concentrated under air. The pale yellow crystals were collected, washed with acetonitrile, and dried in air. Yield: 72 mg (14%).

[Pt₂Ag₄(μ-pz)₈] (5). **Method A.** To a propionitrile solution (40 mL) of [PtCl₂(C₂H₅CN)₂] (145 mg, 0.38 mmol) was added AgPF₆ (254 mg, 1.00 mmol), and the solution was refluxed for 1 h. The solution was cooled to room temperature and filtered to remove the precipitate of AgCl. To the filtrate were added Et₃N (154 mg, 1.52 mmol) and pzH (102 mg, 1.50 mmol), and the solution was

again refluxed for 2 h. After filtration, the filtrate was concentrated under air. The colorless crystals were collected, washed with propionitrile, and dried in air. Yield: 10 mg (4%). The use of 4 equiv of AgPF₆ (420 mg, 1.7 mmol) afforded 15 mg (6%) of **5**. Anal. Calcd for C₂₄H₂₄Ag₄N₁₆Pd₂: C, 21.22; H, 1.78; N, 16.50. Found: C, 21.45; H, 1.86; N, 16.77. ESIMS: *m/z* 1359 ([M + H]⁺).

Method B. A suspension of [Pt(pz)₂(pzH)₂] (**7**) (235 mg, 0.25 mmol) and AgPF₆ (317 mg, 1.3 mmol) in acetonitrile (50 mL) was stirred for 24 h at 20 °C. White solid was collected, washed with acetonitrile, and dried in air. Yield: 177 mg (52%).

Reaction of [PdCl₂(CH₃CN)₂] with pzH in the Absence of Et₃N. To an acetonitrile solution (120 mL) of [PdCl₂(CH₃CN)₂] (130 mg, 0.50 mmol) was added pzH (103 mg, 1.50 mmol), and the solution was stirred for 1 h at 25 °C. No white solid of polymer appeared in this case. The solution was filtered and concentrated under air. The yellow crystals, [Pd(pzH)₄]Cl₂ (**6**), were collected, washed with acetonitrile, and dried in air. Yield: 45 mg (20% based on [PdCl₂(CH₃CN)₂]). An addition of a few drops of water (ca 0.1 mL) to the reacting solution improves the yield (75 mg, 33% ([PdCl₂(CH₃CN)₂]/pzH = 1/3); 176 mg, 77% ([PdCl₂(CH₃CN)₂]/pzH = 1/4)). Since the crystals contain water molecules as solvent of crystallization, the elemental analyses were performed for the powdered samples dried in vacuo. Anal. Calcd for C₁₂H₁₆Cl₂N₈-Pd: C, 32.06; H, 3.59; N, 24.92. Found: C, 32.59; H, 3.92; N, 24.48.

Reaction of [PtCl₂(C₂H₅CN)₂] with pzH in the Presence of Et₃N. To a propionitrile solution (100 mL) of [PtCl₂(C₂H₅CN)₂] (189 mg, 0.50 mmol) were added pzH (103 mg, 1.52 mmol) and Et₃N (155 mg, 1.54 mmol), and the solution was refluxed for 4 h. After filtration, the filtrate was concentrated under air. The colorless crystals, [Pt(pz)₂(pzH)₂] (**7**),⁴³ appeared 2 weeks later and were collected, washed with acetonitrile, and dried in air. Yield: 23 mg (10%). This compound was confirmed by X-ray crystallographic analysis.

Conversion of *trans*-[PtCl₂(pzH)₂] to [Pt₃(μ-pz)₆] in CH₃CN. To an acetonitrile solution (100 mL) of *trans*-[PtCl₂(pzH)₂] (162 mg, 0.40 mmol) was added Et₃N (117 mg, 1.16 mmol), and the solution was refluxed for 6 h. After filtration, the filtrate was concentrated under air. The colorless crystals of [Pt₃(μ-pz)₆] (**8**)³³ were collected, washed with acetonitrile, and dried in vacuo. Yield: 16 mg (12%). This compound was confirmed by X-ray crystallographic analysis (see Supporting Information).

X-ray Structural Determinations. Crystals suitable for X-ray

(43) Burger, W.; Strähle, J. Z. *Anorg. Allg. Chem.* **1986**, *539*, 27.

Table 1. Crystallographic Data for [Pd₃(μ-pz)₆] (**1**), [Pd₃(μ-pz)₆]·2CH₃CN (**1**·2CH₃CN), [Pd₃(μ-4-Mepz)₆]·2CH₃CN (**2**·2CH₃CN), [Pd₂(μ-3-*t*-Bupz)₂(3-*t*-Bupz)₂(3-*t*-BupzH₂)] (**3**), [Pd₂Ag₂(μ-3-*t*-Bupz)₆]·2CH₃CN (**4**·2CH₃CN), [Pt₂Ag₄(μ-pz)₈] (**5**), and [Pd(pzH₄)₄]Cl₂·H₂O (**6**·H₂O)

	1	1 ·2CH ₃ CN	2 ·2CH ₃ CN	3	4 ·2CH ₃ CN	5	6 ·H ₂ O
empirical formula	C ₁₈ H ₁₈ N ₁₂ Pd ₃	C ₂₂ H ₂₄ N ₁₄ Pd ₃	C ₂₈ H ₃₀ N ₁₄ Pd ₃	C ₄₂ H ₆₈ N ₁₂ Pd ₂	C ₄₆ H ₇₂ Ag ₂ N ₁₄ Pd ₂	C ₂₄ H ₂₄ Ag ₄ N ₁₆ Pt ₂	C ₁₂ H ₁₈ Cl ₂ N ₈ OPd
fw	721.62	803.73	881.84	953.88	1249.70	1358.21	467.63
<i>T</i> , K	296	295	133	297	296	295	296
λ , Å	0.71069	0.71069	0.71069	0.71069	0.71069	0.71069	0.71069
cryst syst	tetragonal	monoclinic	orthorhombic	monoclinic	triclinic	triclinic	monoclinic
space group	<i>I</i> ₄ / <i>a</i> (88)	<i>P</i> ₂ / <i>c</i> (14)	<i>Pna</i> 2 ₁ (33)	<i>P</i> ₂ / <i>a</i> (14)	<i>P</i> $\bar{1}$ (2)	<i>P</i> $\bar{1}$ (2)	<i>P</i> ₂ / <i>n</i> (14)
<i>a</i> , Å	16.9731(2)	9.7740(6)	16.107(2)	13.262(1)	12.9227(4)	12.4172(7)	14.303(1)
<i>b</i> , Å	16.9731(2)	8.2355(8)	16.113(2)	21.008(2)	13.737(1)	12.5091(9)	9.949(1)
<i>c</i> , Å	30.6315(7)	33.9192(8)	25.721(3)	18.5598(4)	16.9794(9)	13.921(1)	14.5398(4)
α , deg	90	90	90	90	102.792(2)	96.084(3)	90
β , deg	90	90.0116(5)	90	108.5263(5)	93.4591(8)	105.806(1)	117.0884(5)
γ , deg	90	90	90	90	108.9882(5)	113.7264(8)	90
<i>V</i> , Å ³	8824.5(3)	2730.3(3)	6675(1)	4902.9(6)	2750.6(3)	1846.8(2)	1842.1(3)
<i>Z</i>	16	4	8	4	2	2	4
ρ_{calcd} , Mg m ⁻³	2.172	1.955	1.755	1.292	1.509	2.442	1.686
μ (Mo K α), mm ⁻¹	2.456	1.997	1.643	0.774	1.386	9.629	1.315
no. of unique reflns	5057 (<i>R</i> _{int} = 0.030)	6377 (<i>R</i> _{int} = 0.024)	7612 (<i>R</i> _{int} = 0.021)	11031 (<i>R</i> _{int} = 0.031)	11845 (<i>R</i> _{int} = 0.016)	7838 (<i>R</i> _{int} = 0.034)	3947 (<i>R</i> _{int} = 0.018)
data/restraints/params	5057/0/298	5981/0/352	12056/0/810	11031/0/505	11845/0/577	7838/0/415	3947/0/217
final <i>R</i> indices	<i>R</i> ^a = 0.027	<i>R</i> = 0.023	<i>R</i> = 0.020	<i>R</i> = 0.036	<i>R</i> = 0.027	<i>R</i> = 0.043	<i>R</i> = 0.024
[<i>I</i> > 2 σ (<i>I</i>)]							
<i>R</i> indices (all data)	<i>R</i> ^b = 0.039, <i>R</i> _w ^c = 0.053	<i>R</i> = 0.039, <i>R</i> _w = 0.079	<i>R</i> = 0.032, <i>R</i> _w = 0.058	<i>R</i> = 0.055, <i>R</i> _w = 0.089	<i>R</i> = 0.041, <i>R</i> _w = 0.096	<i>R</i> = 0.078, <i>R</i> _w = 0.124	<i>R</i> = 0.038, <i>R</i> _w = 0.076
GOF	1.04	1.03	0.82	1.02	1.48	1.66	1.07

$$^a R_1 = \sum |F_o| - |F_c| / \sum |F_o|. \quad ^b R = \sum (F_o^2 - F_c^2) / \sum F_o^2. \quad ^c R_w = [\sum [w(F_o^2 - F_c^2)^2] / \sum [w(F_o^2)^2]]^{1/2}.$$

structural analysis were obtained directly from the reaction mixture. The crystals **1**·2CH₃CN, **2**·2CH₃CN, **4**·2CH₃CN, and **6**·H₂O were sealed in thin-walled glass capillaries. The other crystals were mounted on glass fibers. Intensity data were collected on a Quantum CCD area detector coupled with a Rigaku AFC7S diffractometer using graphite-monochromated Mo K α (λ = 0.71069 Å) radiation at 295–297 K. Final cell parameters were obtained from a least-squares analysis of reflections with *I* > 10 σ (*I*). Data were collected in 0.5° oscillations with 30.0 s exposures. A sweep of data was done using ϕ oscillations from 0.0° to 190.0° at χ = 0°, and a second sweep was performed using ω oscillations between –19.0° and 23.0° at χ = 90.0°. The crystal-to-detector distance was 40.7 mm, and the detector swing angle was –5.0°. The data were corrected for Lorentz and polarization effects. An empirical absorption correction was applied.⁴⁴ For **2**·2CH₃CN, intensity data were collected on a Rigaku/MSC Mercury CCD diffractometer using graphite-monochromated Mo K α (λ = 0.71069 Å) radiation at 133 K. Final cell parameters were obtained from a least-squares analysis of reflections with *I* > 10 σ (*I*). The data were collected up to 55.0°. A total of 1200 oscillation images were collected. Sweeps of data were done using ω oscillations in 0.30° step from –70.0° to 110.0° at χ = 45.0° and ϕ = 0.0° and at χ = 45.0° and ϕ = 90.0°. The exposure rate was 10.0 s/deg, and the detector swing angle was 20.1°. The crystal-to-detector distance was 44.5 mm. The data were corrected for Lorentz and polarization effects. The linear absorption coefficient, μ (16.4 cm⁻¹), was applied.

The crystal structures of **1**, **1**·2CH₃CN, **2**·2CH₃CN, and **3** were solved by direct method (SIR92⁴⁵/SIR97⁴⁶). Those of **4**·2CH₃CN, **5**, and **6**·H₂O were solved by heavy-atom method by using DIRDIF.⁴⁷ The positional and thermal parameters of non-H atoms were refined anisotropically by the full-matrix least-squares method.

The minimized function was $\sum w(F_o^2 - F_c^2)^2$, where $w^{-1} = \sigma^{-2}(F_o^2) + (p(\text{Max}(F_o^2, 0) + 2F_c^2)/3)^2$ (p = 0.01 for **1**, 0.039 for **3**, 0.05 for **1**·2CH₃CN, **2**·2CH₃CN, **4**·2CH₃CN, **5**, and **6**·H₂O). Hydrogen atoms bonded to N atoms in the pyrazolate ring in **3** and those of the water molecule in **6**·H₂O were found from the difference synthesis maps. They were included in the refinement with fixed displacement parameters (1.2 times the displacement parameters of the host atom). The rest of the H atoms in all complexes were included at calculated positions with fixed displacement parameters (1.2 times the displacement parameters of the host atom). In the final cycle of the refinement, parameter shifts were less than 0.1 σ . No correction was made for secondary extinction.

All calculations were performed using TEXSAN.⁴⁸ Further crystallographic data are given in Table 1. Listings of selected bond distances and angles are summarized in Tables 2–4 and 6–9. Non-hydrogen atom coordinates, anisotropic thermal parameters, and full listings of bond distances and angles for **1**–**6** are provided as Supporting Information.

Other Measurements. IR spectra were recorded on a Jasco FT/IR-420 infrared spectrophotometer. The ¹H NMR spectra were obtained at 300 MHz with a Varian Gemini 300 spectrometer.

Cyclic voltammetry was performed with a Hokuto HA-301 potentiostat and a Hokuto HB-104 function generator equipped with a Yokokawa 3086 X-Y recorder. The working and the counter electrodes were a platinum disk and a platinum wire, respectively. Cyclic voltammograms were recorded at a scan rate of 50 mV/s. The sample solutions (ca. 1.0 mM) in 0.1 M TBAP–CH₂Cl₂ were deoxygenated with a stream of argon. The reference electrode was Ag/AgCl, and the half-wave potential of Fc⁺/Fc (*E*_{1/2}(Fc⁺/0) vs Ag/AgCl) was +0.50 V.

(44) Jacobson, R. A. *REQABS*, version 1.1. Molecular Structure Corp.: The Woodlands, TX, 1998.

(45) Altomare, A.; Cascarano, G.; Giacovazzo, C.; Guagliardi, A.; Burla, M. C.; Polidori, G.; Camalli, M. *J. Appl. Crystallogr.* **1994**, *27*, 435.

(46) Altomare, A.; Burla, M. C.; Camalli, M.; Cascarano, G. L.; Giacovazzo, C.; Guagliardi, A.; Moliterni, A. G. G.; Polidori, G.; Spagna, R. *J. Appl. Crystallogr.* **1999**, *32*, 115.

(47) Beurskens, P. T.; Admiraal, G.; Beurskens, G.; Bosman, W. P.; de Gelder, R.; Israel, R.; Smits, J. M. M. *The DIRDIF94 Program System*; Technical Report; Crystallography Laboratory, University of Nijmegen: The Netherlands, 1994.

(48) *teXsan: Crystal Structure Analysis Package*; Molecular Structure Corporation: The Woodlands, TX, 1999.

Table 2. Selected Bond Lengths (Å) and Angles (deg) for [Pd₃(μ-pz)₆]**(1)**

Pd1...Pd2	3.0607(4)	Pd2-N22	2.026(3)
Pd1...Pd3	3.0270(4)	Pd2-N51	2.003(3)
Pd2...Pd3	3.0460(3)	Pd2-N61	2.020(3)
Pd1-N11	2.025(3)	Pd3-N32	2.014(3)
Pd1-N21	2.004(3)	Pd3-N42	2.023(3)
Pd1-N31	2.021(3)	Pd3-N52	2.019(3)
Pd1-N41	1.985(3)	Pd3-N62	2.007(3)
Pd2-N12	2.012(3)		
Pd2-Pd1-Pd3	60.044(8)	N32-Pd3-N62	172.9(1)
Pd1-Pd2-Pd3	59.429(8)	N42-Pd3-N52	170.1(1)
Pd1-Pd3-Pd2	60.527(8)	N42-Pd3-N62	91.0(1)
N11-Pd1-N21	87.9(1)	N52-Pd3-N62	89.0(1)
N11-Pd1-N31	171.8(1)	Pd1-N11-N12	115.1(2)
N11-Pd1-N41	92.3(1)	Pd2-N12-N11	115.0(2)
N21-Pd1-N31	90.9(1)	Pd1-N21-N22	115.4(2)
N21-Pd1-N41	172.4(1)	Pd2-N22-N21	114.6(2)
N31-Pd1-N41	87.8(1)	Pd1-N31-N32	114.4(2)
N12-Pd2-N22	87.8(1)	Pd3-N32-N31	114.7(2)
N12-Pd2-N51	172.1(1)	Pd1-N41-N42	114.7(2)
N12-Pd2-N61	92.2(1)	Pd3-N42-N41	114.3(2)
N22-Pd2-N51	90.9(1)	Pd2-N51-N52	114.5(2)
N22-Pd2-N61	171.0(1)	Pd3-N52-N51	115.0(2)
N51-Pd2-N61	87.8(1)	Pd2-N61-N62	113.8(2)
N32-Pd3-N42	88.4(1)	Pd3-N62-N61	115.9(2)
N32-Pd3-N52	90.5(1)		

Table 3. Selected Bond Lengths (Å) and Angles (deg) for [Pd₃(μ-pz)₆]**(1)**·2CH₃CN

Pd1...Pd2	3.0559(3)	Pd2-N22	2.015(3)
Pd1...Pd3	3.0560(3)	Pd2-N51	2.021(3)
Pd2...Pd3	3.0293(4)	Pd2-N61	2.011(3)
Pd1-N11	2.010(3)	Pd3-N32	2.016(3)
Pd1-N21	2.024(3)	Pd3-N42	2.020(3)
Pd1-N31	2.023(3)	Pd3-N52	2.019(3)
Pd1-N41	2.011(3)	Pd3-N62	2.011(3)
Pd2-N12	2.019(3)		
Pd2-Pd1-Pd3	59.424(8)	N32-Pd3-N62	173.0(1)
Pd1-Pd2-Pd3	60.289(8)	N42-Pd3-N52	170.7(1)
Pd1-Pd3-Pd2	60.287(8)	N42-Pd3-N62	92.3(1)
N11-Pd1-N21	87.8(1)	N52-Pd3-N62	88.7(1)
N11-Pd1-N31	171.2(1)	Pd1-N11-N12	115.6(2)
N11-Pd1-N41	90.7(1)	Pd2-N12-N11	114.3(2)
N21-Pd1-N31	92.2(1)	Pd1-N21-N22	113.9(2)
N21-Pd1-N41	171.3(1)	Pd2-N22-N21	115.9(2)
N31-Pd1-N41	87.9(1)	Pd1-N31-N32	114.2(2)
N12-Pd2-N22	88.0(1)	Pd3-N32-N31	115.5(2)
N12-Pd2-N51	170.6(1)	Pd1-N41-N42	115.6(2)
N12-Pd2-N61	92.2(1)	Pd3-N42-N41	114.1(2)
N22-Pd2-N51	90.0(1)	Pd2-N51-N52	114.6(2)
N22-Pd2-N61	172.9(1)	Pd3-N52-N51	114.8(2)
N51-Pd2-N61	88.7(1)	Pd2-N61-N62	114.7(2)
N32-Pd3-N42	88.1(1)	Pd3-N62-N61	114.6(2)
N32-Pd3-N52	89.8(1)		

Results and Discussion

Synthesis and Characterization. Pyrazolato-bridged cyclic trinuclear Pd(II) complex **1** has been prepared by the reaction of [PdCl₂(CH₃CN)₂] with pyrazole in the presence of Et₃N at room temperature. 4-Methylpyrazole also gave cyclic trinuclear complex **2**. In these reactions, as well as the reaction of the Pt analogue,³³ the formation of trinuclear complexes competes with that of polymeric species ([Pd-(Rpz)₂]_n). Thus the reaction in dilute solution containing the Pd(II) ion and pyrazole afforded the trinuclear complex in higher yield (Scheme 1): the yield of **1** was improved more than three times as the amount of solvent increased from 30 mL to 200 mL. Because the formation of polymeric species

Table 4. Selected Bond Lengths (Å) and Angles (deg) for [Pd₃(μ-4-Mepz)₆]**(2)**·2CH₃CN

Pd1...Pd2	3.0595(4)	Pd3-N42	2.013(3)
Pd1...Pd3	3.0562(4)	Pd3-N52	2.000(3)
Pd2...Pd3	3.0486(4)	Pd3-N62	2.014(3)
Pd4...Pd5	3.0727(4)	Pd4-N71	2.015(3)
Pd4...Pd6	3.0494(4)	Pd4-N81	2.012(3)
Pd5...Pd6	3.0433(4)	Pd4-N91	2.031(3)
Pd1-N11	2.022(3)	Pd4-N101	2.010(3)
Pd1-N21	2.011(3)	Pd5-N72	2.010(3)
Pd1-N31	2.021(3)	Pd5-N82	2.015(3)
Pd1-N41	2.017(3)	Pd5-N111	2.023(3)
Pd2-N12	2.029(3)	Pd5-N121	2.022(3)
Pd2-N22	2.016(3)	Pd6-N92	1.999(3)
Pd2-N51	2.020(3)	Pd6-N102	2.014(3)
Pd2-N61	2.026(3)	Pd6-N112	2.013(3)
Pd3-N32	2.021(3)	Pd6-N122	2.012(3)
Pd2-Pd1-Pd3	59.799(9)	N82-Pd5-N111	93.9(1)
Pd1-Pd2-Pd3	60.047(9)	N82-Pd5-N121	172.0(1)
Pd1-Pd3-Pd2	60.154(9)	N111-Pd5-N121	86.9(1)
Pd5-Pd4-Pd6	59.616(9)	N92-Pd6-N102	87.9(1)
Pd4-Pd5-Pd6	59.811(9)	N92-Pd6-N112	92.4(1)
Pd4-Pd6-Pd5	60.573(9)	N92-Pd6-N122	171.1(1)
N11-Pd1-N21	88.9(1)	N102-Pd6-N112	173.3(1)
N11-Pd1-N31	171.3(1)	N102-Pd6-N122	92.0(1)
N11-Pd1-N41	90.4(1)	N112-Pd6-N122	86.7(1)
N21-Pd1-N31	90.0(1)	Pd1-N11-N12	114.8(2)
N21-Pd1-N41	171.7(1)	Pd2-N12-N11	114.8(2)
N31-Pd1-N41	89.4(1)	Pd1-N21-N22	114.4(2)
N12-Pd2-N22	87.7(1)	Pd2-N22-N21	115.5(2)
N12-Pd2-N51	171.8(1)	Pd1-N31-N32	114.1(2)
N12-Pd2-N61	93.2(1)	Pd3-N32-N31	115.4(2)
N22-Pd2-N51	90.8(1)	Pd1-N41-N42	114.3(2)
N22-Pd2-N61	171.8(1)	Pd3-N42-N41	115.2(2)
N51-Pd2-N61	87.2(1)	Pd2-N51-N52	114.4(2)
N32-Pd3-N42	88.2(1)	Pd3-N52-N51	115.2(2)
N32-Pd3-N52	91.4(1)	Pd2-N61-N62	113.6(2)
N32-Pd3-N62	173.0(1)	Pd3-N62-N61	115.4(2)
N42-Pd3-N52	171.0(1)	Pd4-N71-N72	115.3(2)
N42-Pd3-N62	92.6(1)	Pd5-N72-N71	115.0(2)
N52-Pd3-N62	86.7(1)	Pd4-N81-N82	115.2(2)
N71-Pd4-N81	87.9(1)	Pd5-N82-N81	115.1(2)
N71-Pd4-N91	170.0(1)	Pd4-N91-N92	113.2(2)
N71-Pd4-N101	90.4(1)	Pd6-N92-N91	116.3(2)
N81-Pd4-N91	92.2(1)	Pd4-N101-N102	114.4(2)
N81-Pd4-N101	172.4(1)	Pd6-N102-N101	115.3(2)
N91-Pd4-N101	88.2(1)	Pd5-N111-N112	113.1(2)
N72-Pd5-N82	87.8(1)	Pd6-N112-N111	116.1(2)
N72-Pd5-N111	171.5(1)	Pd5-N121-N122	114.5(2)
N72-Pd5-N121	90.2(1)	Pd6-N122-N121	114.8(2)

prevails over the formation of the trimeric species under higher concentration, the isolation of pyrazolato-bridged trinuclear Pd(II) complex may have not been successful despite a large number of reactions conducted.^{49,50}

On the contrary, the reaction of Pd(II) ion with pyrazole in the absence of Et₃N afforded a mononuclear complex, [Pd(pzH)₄]Cl₂ (**6**), consisting of Pd(II) ion, neutral pyrazole ligands, and outer-sphere chloride ions.^{42,50} Treatment of the mononuclear complex **6** with Et₃N afforded the cyclic trinuclear complex **1** in higher yield than the direct synthesis.

Complex **1** does not exhibit an oxidation process up to +1.9 V, which is in contrast with the expectation that **1** may be oxidized easily due to the electronic repulsion of d_{z²} orbitals spatially oriented toward the center of the triangle. However, **2** exhibits an irreversible oxidation process at

(49) Minghetti, G.; Banditelli, G.; Bonati, F. *J. Chem. Soc., Dalton Trans.* **1979**, 1851.

(50) Ardizzoia, G. A.; La Monica, G.; Cenini, S.; Moret, M.; Masciocchi, N. *J. Chem. Soc., Dalton Trans.* **1996**, 1351.

Table 5. Comparison of Important Structural Parameters^a

	[Pd ₃ (μ-pz) ₆] (1) ^b	[Pd ₃ (μ-4-Mepz) ₆] (2) ^b	[Pd ₃ (μ-Phpz) ₆] ^c	[Pt ₃ (μ-pz) ₆] ^d	[Pd ₃ (μ-OAc) ₆] ^e
M···M (av), Å	3.0471[126]	3.0548[46]	3.0541[407]	3.048[14]	3.140[41]
M–N/O (av), Å	2.017[5]	2.018[7]	2.002[17]	2.011[11]	1.99[1]
M–M–N/O (av), deg	65.18[20]	65.19[25]	65.0[11]		76.3[13]
M–N–N (av), deg	114.8[6]	114.8[6]	114.9[19]		
M–O–C (av), deg					129.6[22]

^a Numbers in square brackets are root-mean-square deviations of the individual values from their mean. ^b Acetonitrile solvate. ^c Reference 34. ^d Reference 33. ^e Reference 38.

Table 6. Selected Bond Lengths (Å) and Angles (deg) for [Pd₂(μ-3-*t*-Bupz)₂(3-*t*-Bupz)₂(3-*t*-BupzH₂)] (3)

Pd1···Pd2	3.1758(4)	Pd2–N11	2.018(3)
Pd1–N12	2.012(2)	Pd2–N22	2.015(2)
Pd1–N21	2.017(2)	Pd2–N51	2.013(3)
Pd1–N31	2.021(3)	Pd2–N61	2.036(2)
Pd1–N41	2.020(3)		
N12–Pd1–N21	85.28(10)	N22–Pd2–N61	177.2(1)
N12–Pd1–N31	176.27(10)	N51–Pd2–N61	92.5(1)
N12–Pd1–N41	89.3(1)	Pd2–N11–N12	115.7(2)
N21–Pd1–N31	91.35(10)	Pd1–N12–N11	114.9(2)
N21–Pd1–N41	173.4(1)	Pd1–N21–N22	115.9(2)
N31–Pd1–N41	94.2(1)	Pd2–N22–N21	115.1(2)
N11–Pd2–N22	85.73(10)	Pd1–N31–N32	123.1(2)
N11–Pd2–N51	174.6(1)	Pd1–N41–N42	124.7(2)
N11–Pd2–N61	91.7(1)	Pd2–N51–N52	123.2(2)
N22–Pd2–N51	90.1(1)	Pd2–N61–N62	122.3(2)

Table 7. Selected Bond Lengths (Å) and Angles (deg) for [Pd₂Ag₂(μ-3-*t*-Bupz)₆]·2CH₃CN (4·2CH₃CN)

Ag1···Ag2	4.5909(3)	Ag2···Pd1	3.5149(3)
Ag1···Pd1	3.4949(3)	Ag2···Pd2	3.3414(3)
Ag1···Pd2	3.2635(3)	Pd1···Pd2	3.3801(3)
Ag1–N32	2.099(2)	Pd1–N31	2.026(2)
Ag1–N52	2.116(2)	Pd1–N41	2.020(2)
Ag2–N42	2.106(2)	Pd2–N11	2.005(2)
Ag2–N62	2.124(2)	Pd2–N21	1.997(2)
Pd1–N12	2.054(2)	Pd2–N51	2.007(2)
Pd1–N22	2.049(2)	Pd2–N61	2.017(2)
N32–Ag1–N52	173.02(9)	N51–Pd2–N61	90.7(1)
N42–Ag2–N62	175.4(1)	N12–N11–Pd2	125.7(2)
N12–Pd1–N22	88.59(9)	N11–N12–Pd1	112.5(2)
N12–Pd1–N31	177.38(9)	N22–N21–Pd2	125.9(2)
N12–Pd1–N41	91.06(9)	N21–N22–Pd1	113.7(2)
N22–Pd1–N31	91.58(9)	N32–N31–Pd1	122.2(2)
N22–Pd1–N41	178.61(9)	N31–N32–Ag1	120.0(2)
N31–Pd1–N41	88.7(1)	N42–N41–Pd1	123.6(2)
N11–Pd2–N21	90.92(9)	N41–N42–Ag2	118.8(2)
N11–Pd2–N51	176.30(9)	N52–N51–Pd2	121.7(2)
N11–Pd2–N61	90.1(1)	N51–N52–Ag1	112.8(2)
N21–Pd2–N51	88.1(1)	N62–N61–Pd2	122.5(2)
N21–Pd2–N61	177.01(9)	N61–N62–Ag2	114.6(2)

+1.71 V. The difference of **1** and **2** in the redox behavior is attributed to the influence of the substituent group on the pyrazolate ring.

The trimeric Pt analogue can be prepared from two different starting materials: one is the dimer of the neutral mononuclear complex [Pt(pz)₂(pzH)₂]₂ (**7**), with intermolecular hydrogen bonding, and the other is *trans*-[PtCl₂(pzH)₂], without hydrogen bonding. Burger and Strähle have reported that the preparation of the cyclic trinuclear Pt(II) complex, [Pt₃(μ-pz)₆] (**8**), from **7** needs heating at a high temperature such as 185 °C in mesitylene.³³ We have conducted the reaction under the same conditions as those in their report and have confirmed that the use of a sealed tube is more efficient for the formation of **8** than the simple

Table 8. Selected Bond Lengths (Å) and Angles (deg) for [Pt₂Ag₄(μ-pz)₈] (5)

Pt1···Pt2	5.1720(3)	Ag1···Ag3	4.8133(9)
Pt1···Ag1	3.5386(6)	Ag1···Ag4	3.4427(9)
Pt1···Ag2	3.5578(7)	Ag2···Ag3	3.3578(9)
Pt1···Ag3	3.5545(6)	Ag2···Ag4	4.747(1)
Pt1···Ag4	3.4728(6)	Ag3···Ag4	3.2981(8)
Pt2···Ag1	3.5393(6)	N12···N52	4.198(9)
Pt2···Ag2	3.4846(7)	N22···N62	4.18(1)
Pt2···Ag3	3.4981(6)	N32···N72	4.217(9)
Pt2···Ag4	3.5273(6)	N42···N82	4.196(9)
Ag1···Ag2	3.4237(9)		
Pt1–N11	2.012(6)	Ag1–N12	2.092(6)
Pt1–N21	2.004(7)	Ag1–N52	2.108(7)
Pt1–N31	1.996(6)	Ag2–N22	2.088(7)
Pt1–N41	2.029(7)	Ag2–N62	2.096(7)
Pt2–N51	2.014(6)	Ag3–N32	2.108(6)
Pt2–N61	1.992(6)	Ag3–N72	2.110(6)
Pt2–N71	2.014(6)	Ag4–N42	2.108(6)
Pt2–N81	2.006(6)	Ag4–N82	2.090(6)
N11–Pt1–N21	90.6(2)	Pt1–N11–N12	121.4(5)
N11–Pt1–N31	179.4(2)	Ag1–N12–N11	122.7(4)
N11–Pt1–N41	89.7(2)	Pt1–N21–N22	121.7(5)
N21–Pt1–N31	89.8(2)	Ag2–N22–N21	123.3(5)
N21–Pt1–N41	179.1(2)	Pt1–N31–N32	122.4(5)
N31–Pt1–N41	89.8(2)	Ag3–N32–N31	122.1(5)
N51–Pt2–N61	89.4(3)	Pt1–N41–N42	121.7(5)
N51–Pt2–N71	178.8(2)	Ag4–N42–N41	120.0(5)
N51–Pt2–N81	90.3(2)	Pt2–N51–N52	121.9(5)
N61–Pt2–N71	90.9(3)	Ag1–N52–N51	121.5(5)
N61–Pt2–N81	179.2(2)	Pt2–N61–N62	121.7(5)
N71–Pt2–N81	89.3(2)	Ag2–N62–N61	120.9(5)
N12–Ag1–N52	176.1(2)	Pt2–N71–N72	121.9(5)
N22–Ag2–N62	174.5(3)	Ag3–N72–N71	120.6(5)
N32–Ag3–N72	176.9(2)	Pt2–N81–N82	120.8(4)
N42–Ag4–N82	176.1(2)	Ag4–N82–N81	122.8(4)

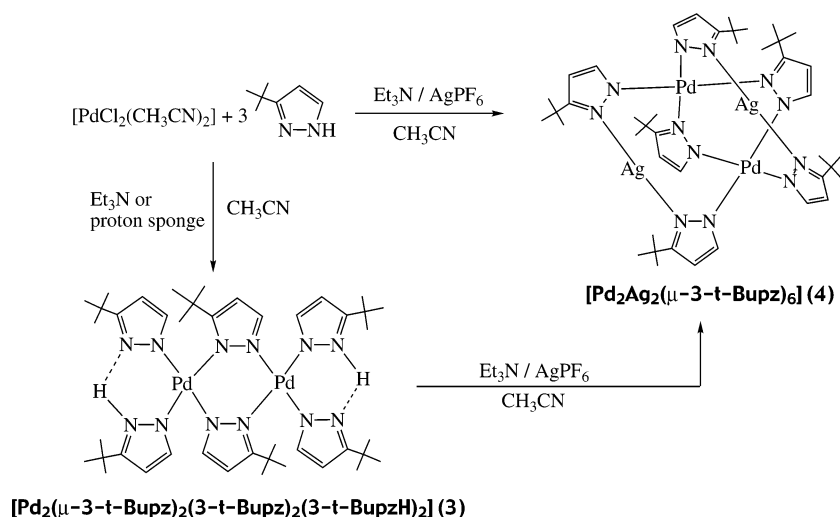
Table 9. Selected Bond Lengths (Å) and Angles (deg) for [Pd(pzH)₄]Cl₂·H₂O (6·H₂O)

Pd1–N11	2.013(2)	Pd1–N31	2.015(2)
Pd1–N21	2.009(2)	Pd1–N41	2.005(2)
N11–Pd1–N21	89.68(7)	N21–Pd1–N31	89.94(7)
N11–Pd1–N31	178.51(6)	N21–Pd1–N41	179.27(6)
N11–Pd1–N41	89.61(8)	N31–Pd1–N41	90.77(7)

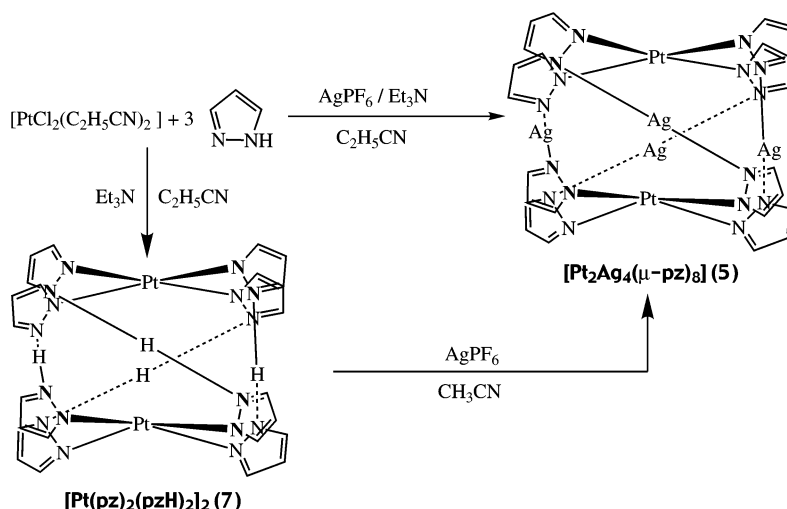
refluxing of **7** in mesitylene under an ambient pressure of argon atmosphere (24% yield for the reaction in a sealed tube and 5% yield for the latter; see Supporting Information). The reaction of [PtCl₂(C₂H₅CN)₂] with pyrazole in the presence of Et₃N under refluxing in C₂H₅CN merely afforded **7**. However, we have found that **8** forms in higher yield than the case of simple refluxing of **7** in mesitylene when *trans*-[PtCl₂(pzH)₂] was refluxed in CH₃CN in the presence of Et₃N.

Although a cyclic trinuclear Pd(II) complex, [Pd₃(μ-3-Phpz)₆] (3-Phpz = 3-phenylpyrazolate), has been prepared by a stepwise manner via an open-chain trimer [Pd₃(μ-3-Phpz)₄(3-PhpzH)₂Cl₂],³⁴ an attempt to prepare a trinuclear

Scheme 2



Scheme 3



complex with 3-*t*-Bupz failed, probably due to steric hindrance of the bulky substituent at the 3-position of the pyrazolato ring. Consequently, a dinuclear Pd(II) complex having both anionic bridging ligands and neutral terminal ligands, $[\text{Pd}_2(\mu\text{-3-}t\text{-Bupz})_2(3\text{-}t\text{-Bupz})_2(3\text{-}t\text{-BupzH})_2]$ (**3**), was obtained in the reaction of Pd(II) ion with 3-*t*-BupzH in the presence of Et_3N or Proton Sponge. The apparent low yield of the product is attributed to the difficulty in the isolation of the pure product due to the contamination of Et_3NHCl . Thus the pure complex **3** was collected in a crystalline form before Et_3NHCl started to precipitate.

The abstraction of the protons participating in the hydrogen bonding by bases was not successful toward **3** and **7**. However, mixed-metal complexes $[\text{Pd}_2\text{Ag}_2(\mu\text{-3-}t\text{-Bupz})_6]$ (**4**) and $[\text{Pt}_2\text{Ag}_4(\mu\text{-pz})_8]$ (**5**) readily formed by addition of Ag^+ ions to **3** and **7**, respectively (Schemes 2 and 3). Facile replacement of protons by Ag^+ ions is known for $[\text{Pd}(\text{dmpz})_2\text{-}(\text{dmpzH})_2]_2$ to give $[\text{Pd}_2\text{Ag}_4(\mu\text{-dmpz})_8]$.⁵⁰

The reaction of $[\text{PdCl}(\text{tropolonate})(\text{CH}_3\text{CN})]$ with $\text{K}\{\text{B}(3\text{-}t\text{-Bupz})_4\}$ in CH_3CN gave **3** accompanied by the B–N bond cleavage of $\{\text{B}(3\text{-}t\text{-Bupz})_4\}^-$ and by the successive proton abstraction probably from the water molecules in the solution. The B–N bond cleavage of $\{\text{B}(3\text{-}t\text{-Bupz})_4\}^-$ also

occurred when $[\text{PdCl}_2(\text{CH}_3\text{CN})_2]$ was employed as a starting material. The use of nonsubstituted pyrazolylborate, $\{\text{B}(\text{pz})_4\}^-$, however, afforded $[\text{Pd}\{\text{B}(\text{pz})_4\}_2]$ as a major product without accompanying B–N bond cleavage of the borate. It is unclear at this stage whether steric bulkiness or electronic effect of the *tert*-butyl group is the main factor of B–N bond cleavage.

Crystal Structures. X-ray structural analyses of **1–6** were performed. The cyclic trinuclear Pd(II) complex with nonsubstituted pyrazolate, $[\text{Pd}_3(\mu\text{-pz})_6]$ (**1**) (Figure 1), crystallized in two different space groups, $I4_1/a$ and $P2_1/c$, corresponding to the absence and presence of the solvent of crystallization, respectively. The former is isomorphous to $[\text{Pt}_3(\mu\text{-pz})_6]$ (**8**).³³ Although the molecular structures of complex **1** in both space groups are almost the same, the observation of small but apparent differences in the metal–metal distances is worth remarking on. The ideally equilateral triangle molecule distorts to an isosceles triangle in $1 \cdot 2\text{CH}_3\text{CN}$ ($\text{Pd1}\cdots\text{Pd2} = 3.0559(3) \text{ \AA}$, $\text{Pd1}\cdots\text{Pd3} = 3.0560(3) \text{ \AA}$, $\text{Pd2}\cdots\text{Pd3} = 3.0293(4) \text{ \AA}$), while the regularity in Pd \cdots Pd distances is not found in the crystal of **1** ($\text{Pd1}\cdots\text{Pd2} = 3.0607(4) \text{ \AA}$, $\text{Pd1}\cdots\text{Pd3} = 3.0270(4) \text{ \AA}$, $\text{Pd2}\cdots\text{Pd3} = 3.0460(3) \text{ \AA}$). In both **1** and $1 \cdot 2\text{CH}_3\text{CN}$, the complex molecule has an approximate 3-fold axis at the center of the molecule perpendicular to the plane

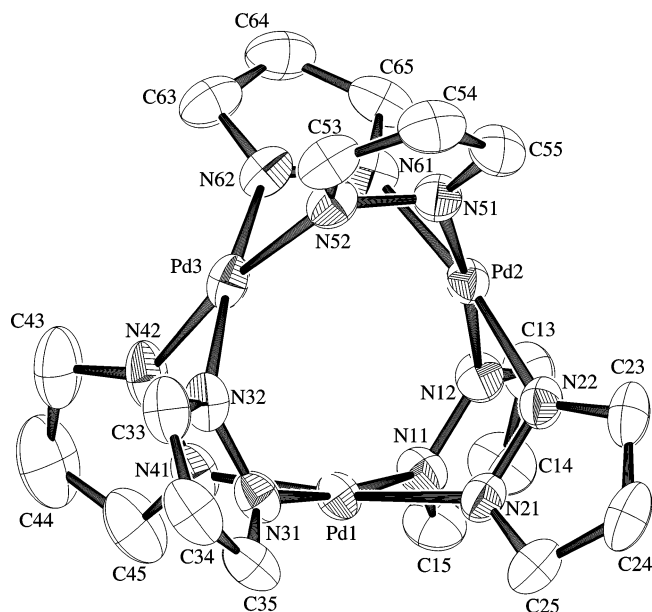


Figure 1. Molecular structure of $[\text{Pd}_3(\mu\text{-pz})_6]$ (**1**) with the atom-numbering scheme (50% probability ellipsoids).

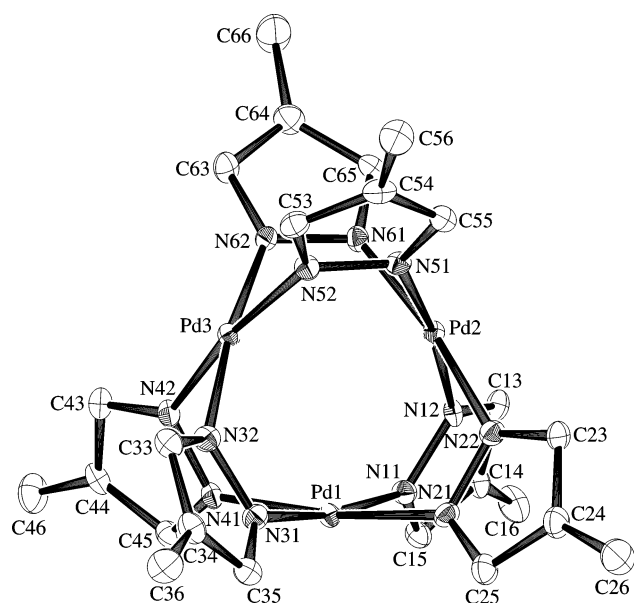
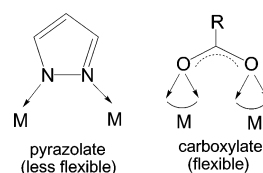


Figure 2. Molecular structure of $[\text{Pd}_3(\mu\text{-4-Mepz})_6]$ (**2**) with the atom-numbering scheme (50% probability ellipsoids).

defined by three Pd atoms. The Pd–N distances and N–Pd–N angles are in the ranges 1.985(3)–2.026(3) Å and 87.8(1)–92.3(1)°, respectively.

The 4-methylpyrazolato-bridged cyclic trinuclear Pd(II) complex, $[\text{Pd}_3(\mu\text{-4-Mepz})_6]$ (**2**), crystallized in orthorhombic $Pna2_1$ as an acetonitrile solvate. Because the asymmetric unit of **2** consists of two crystallographically independent molecules, one of them is illustrated in Figure 2. The structure of the complex molecule is very similar to that of **1** except for the existence of methyl groups on the pyrazolate rings. Both of the independent complex molecules in **2** also distorted to isosceles triangles (molecule 1, Pd1⋯Pd2 = 3.0595(4) Å, Pd1⋯Pd3 = 3.0562(4) Å, Pd2⋯Pd3 = 3.0486(4) Å; molecule 2, Pd4⋯Pd5 = 3.0727(4) Å, Pd4⋯Pd6 = 3.0494(4) Å, Pd5⋯Pd6 = 3.0433(3) Å).

Chart 1



Because the structures of complex molecules in **1** and **2** as well as $[\text{Pt}_3(\mu\text{-pz})_6]$ (**8**) are similar to that of palladium acetate, $[\text{Pd}_3(\mu\text{-OAc})_6]$, it is worthwhile to compare these structures (Charts 1 and 2, Table 5). The average metal–metal distances of **1**, **2**, **8**, and $[\text{Pd}_3(\mu\text{-Phpz})_6]$ are very similar to one another, though the values of the root-mean-square deviations in **1**, **2**, and **8** are smaller than that of $[\text{Pd}_3(\mu\text{-Phpz})_6]$. It means that the deviations from the equilateral triangle in **1**, **2**, and **8** are smaller than that in $[\text{Pd}_3(\mu\text{-Phpz})_6]$. Similar distortion to the isosceles triangle can be seen in the structures of $[\text{Pd}_3(\mu\text{-OAc})_6]$ in some cases,^{39,51} though the effect of distortion was attributed to intermolecular packing forces due to the apparent softness of the molecular framework.^{51,52} The average metal–metal distances in **1**, **2**, **8**, and $[\text{Pd}_3(\mu\text{-Phpz})_6]$ are, however, ca. 0.1 Å shorter than that of $[\text{Pd}_3(\mu\text{-OAc})_6]$. Because the average M–N distances in **1**, **2**, and $[\text{Pd}_3(\mu\text{-Phpz})_6]$ are comparable to the average M–O distance in $[\text{Pd}_3(\mu\text{-OAc})_6]$, the N–N distances in pz ligands (ca. 1.35 Å) and the O⋯O distances in OAc ligands (ca. 2.21 Å) mainly affect the average M–M–N (**1**, 65.2°; **2**, 65.2°; $[\text{Pd}_3(\mu\text{-Phpz})_6]$, 65.0°) and M–M–O ($[\text{Pd}_3(\mu\text{-OAc})_6]$, 76.3°) angles, respectively. The apparent magnitude of strain of the trinuclear unit may be estimated by the deviations of the M–N–N ($\Delta = 11^\circ$) and M–O–C ($\Delta = 10^\circ$) angles from the expected values (126° for M–N–N and 120° for M–O–C angles) for the monodentate coordination of pz and OAc ligands to the metal ions through N and O atoms, respectively. It indicates that the apparent magnitude of strain of the trinuclear unit in **1**, **2**, or $[\text{Pd}_3(\mu\text{-Phpz})_6]$ does not so much differ from that in $[\text{Pd}_3(\mu\text{-OAc})_6]$.

The mononuclear complex $[\text{Pd}(\text{pzH})_4]\text{Cl}_2$ (**6**) crystallized in a form of water solvate. The platinum analogue, $[\text{Pt}(\text{pzH})_4]\text{Cl}_2$, has also been reported as a water solvate.⁴² The crystal structure of **6** is shown in Figure S3 (see Supporting Information). Four neutral pyrazole ligands coordinate to the Pd(II) ion in a monodentate fashion with accompanying protons on the N atoms uncoordinated to the Pd atom. The three (H12, H22 and H42) and one (H32) of the four N–H protons form hydrogen bonding to the Cl[−] ion and O atom in the H₂O molecule, respectively, in the crystal structure. There is no intermolecular contact through hydrogen bonding between adjacent $[\text{Pd}(\text{pzH})_4]^{2+}$ units. The Pd–N distances are in the range 2.005(2)–2.015(2) Å and are comparable to those of **1**.

Figure 3 illustrates the structure of the dinuclear complex $[\text{Pd}_2(\mu\text{-3-}t\text{-Bupz})_2(3\text{-}t\text{-BupzH})_2]$ (**3**). The complex molecule has a 2-fold axis at the center of the molecule

(51) Cotton, F. A.; Han, S. *Rev. Chim. Miner.* **1985**, *22*, 277.

(52) Bancroft, D. P.; Cotton, F. A.; Falvello, L. R.; Schwotzer, W. *Polyhedron* **1988**, *7*, 615.

Chart 2

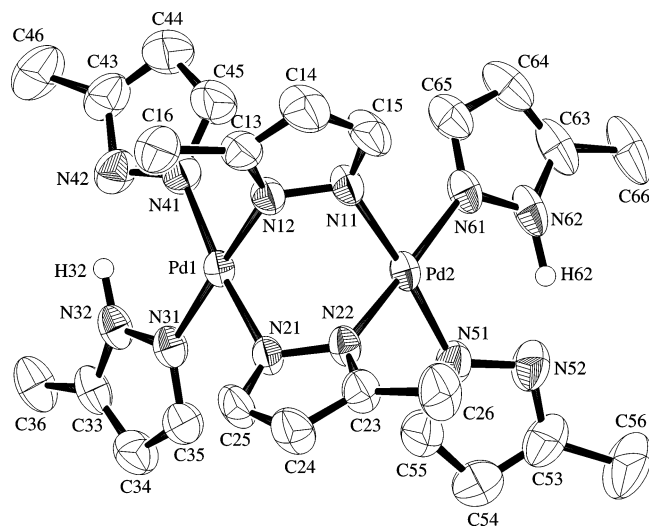
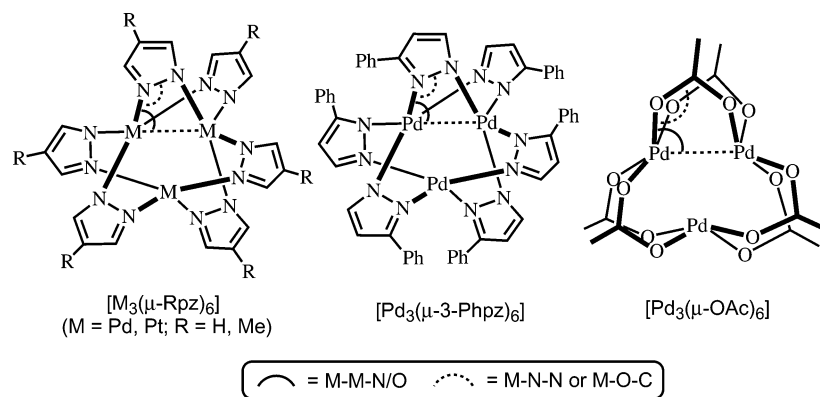


Figure 3. Molecular structure of $[Pd_2(\mu\text{-3-}t\text{-Bupz})_2(3\text{-}t\text{-BupzH})_2]$ (**3**) with the atom-numbering scheme (50% probability ellipsoids). Methyl carbon atoms in *tert*-butyl groups have been omitted for clarity.

normal to the Pd...Pd axis; therefore the $Pd_2(\mu\text{-3-}t\text{-Bupz})_2$ unit has the *head-to-tail* configuration. Two of the four terminal monodentate ligands are the 3-*t*-Bupz anion, and the rest of the ligands are neutral 3-*t*-BupzH. The neutral 3-*t*-BupzH ligands form hydrogen bonds with adjacent anionic 3-*t*-Bupz ligands (pz3–H32...pz4, pz5...H62–pz6). The hydrogen atoms participating in the hydrogen bonding were found from the difference Fourier synthesis map of non-hydrogen atoms. The Pd...Pd separation is 3.1758(4) Å. The Pd–N distances range from 2.012(2) to 2.036(2) Å, indicating that the bridging pyrazolate, terminal pyrazolate, and terminal pyrazole ligands bind to the Pd atom with similar Pd–N distances. The N–Pd–N angles between bridging pyrazolates (N12–Pd1–N21, 85.28(10)°; N11–Pd2–N22, 85.73(10)°) are smaller than those between terminal ligands (N31–Pd1–N41, 94.2(1)°; N51–Pd2–N61, 92.5(1)°), because no strain exists for terminal monodentate ligands.

The molecular structure of the tetranuclear Pd/Ag complex $[Pd_2Ag_2(\mu\text{-3-}t\text{-Bupz})_6]$ (**4**) is shown in Figure 4. The complex molecule has an idealized mirror plane defined by two Pd atoms and the midpoint of Ag...Ag contact, which is consistent with the observation of the existence of three inequivalent 3-*t*-Bupz ligands by ^1H NMR. Replacement of protons participating in the hydrogen bonding in **3** by Ag^+

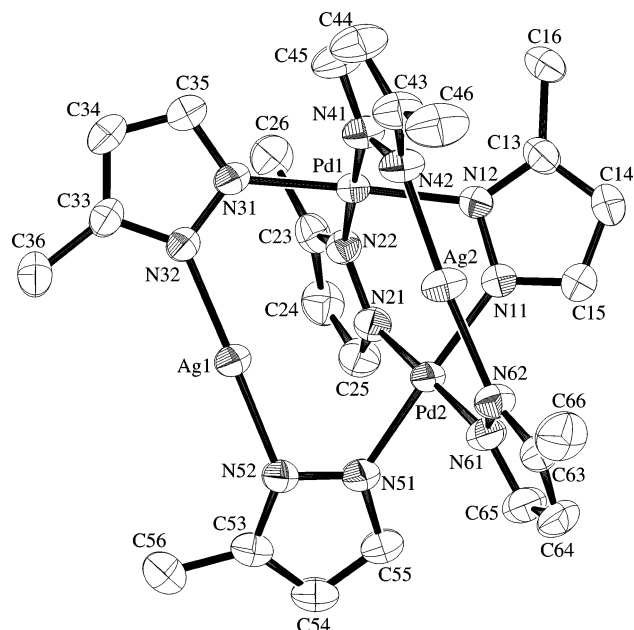


Figure 4. Molecular structure of $[Pd_2Ag_2(\mu\text{-3-}t\text{-Bupz})_6]$ (**4**) with the atom-numbering scheme (50% probability ellipsoids). Methyl carbon atoms in *tert*-butyl groups have been omitted for clarity.

ions leads to the formation of two large fused triangles with a change in the configuration of the $Pd_2(\mu\text{-3-}t\text{-Bupz})_2$ unit from *head-to-tail* to *head-to-head*. One large triangle comprises pz1, pz3, and pz5 rings, and the other comprises pz2, pz4, and pz6 rings. Here, it is worthwhile to note that the Ag^+ ions sit between pz3 and pz5 rings and between pz4 and pz6 rings in **4** instead of the positions occupied by bridging hydrogen atoms in **3**. The nonbonded metal–metal contacts are listed in Table 7. The Pd...Pd separation in **4** (3.3801(3) Å) is elongated by 0.2 Å from that in **3**, owing to the steric requirement by the coordination of pz rings to Ag^+ ions. The Ag1/Ag2...Pd2 distances are ca. 0.2 Å longer than Ag1/Ag2...Pd1 distances, probably due to the steric repulsion between large substituents on the pyrazolate rings. The influence of the steric repulsion is also seen in the Pd–N distances in **4**; the Pd1–N12 and Pd1–N22 distances (2.054(2), 2.049(2) Å) are ca. 0.05 Å longer than Pd2–N11 and Pd2–N21 distances (2.005(2), 1.997(2) Å). The N–Ag–N angles are 173.02(9)° and 175.4(1)°, which are not so much deviated from linear coordination. Because the ionic radius

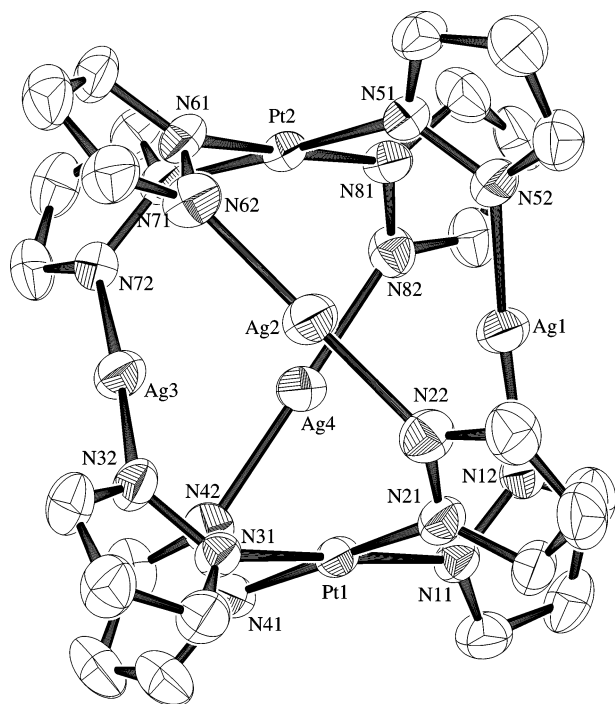


Figure 5. Molecular structure of $[\text{Pt}_2\text{Ag}_4(\mu\text{-pz})_8]$ (**5**) with the atom-numbering scheme (50% probability ellipsoids).

of Ag^+ ion is longer than that of Pd^{2+} ion, the $\text{Ag}-\text{N}$ distances are ca. 0.1 Å longer than the nonstrained $\text{Pd}-\text{N}$ distances.

Replacement of the four bridging hydrogen atoms in the dimer of **7** with Ag^+ ions leads to the formation of the hexanuclear Pt/Ag complex $[\text{Pt}_2\text{Ag}_4(\mu\text{-pz})_8]$ (**5**) (Figure 5). Because the nature of this reaction is essentially the same as that observed for $[\text{Pd}(\text{dmpz})_2(\text{dmpzH})_2]_2$ ⁵⁰ and the structure of **5** is similar to that of $[\text{Pd}_2\text{Ag}_4(\mu\text{-dmpz})_8]$,⁵⁰ it is worth comparing these structures. The complex molecule has idealized 422 (D_4) symmetry, with the 4-fold axis passing through the Pt atoms and two different sets of 2-fold axes normal to it. The $\text{Pt}\cdots\text{Ag}$ distances in **5** are close to one another, ranging from 3.4728(6) to 3.5578(7) Å (Table 8). Because the $\text{Pt1}\cdots\text{Pt2}$ distance (5.1720(3) Å) in **5** is ca. 0.35 Å longer than $\text{Ag1}\cdots\text{Ag3}$ and $\text{Ag2}\cdots\text{Ag4}$ distances (4.8133(9), 4.747(1) Å) in **5**, the Pt_2Ag_4 core can be regarded as a distorted octahedron. These $\text{M}\cdots\text{M}$, $\text{M}\cdots\text{Ag}$, and $\text{Ag}\cdots\text{Ag}$ distances in **5** ($\text{M} = \text{Pt}$) are close to the corresponding distances ($\text{M} = \text{Pd}$) in $[\text{Pd}_2\text{Ag}_4(\mu\text{-dmpz})_8]$ ($\text{Pd}\cdots\text{Pd}$, 5.160(1) Å; $\text{Pd}\cdots\text{Ag}$, 3.465(1)–3.535(1) Å; $\text{Ag}\cdots\text{Ag}$, 3.306(1)–3.426(1) Å). The $\text{N}\cdots\text{N}$ distances (4.18(1)–4.217(9) Å) related to the $\text{N}-\text{Ag}-\text{N}$ bonds in **5** are also close to those in $[\text{Pd}_2\text{Ag}_4(\mu\text{-dmpz})_8]$ (4.152(4)–4.161(5) Å). The $\text{N}-\text{Ag}-\text{N}$ angles in **5** range from 174.5(3)° to 176.9(2)°, which are not so much deviated from linear coordination. These

structural similarities between **7** and $[\text{Pd}(\text{dmpz})_2(\text{dmpzH})_2]_2$ and between **5** and $[\text{Pd}_2\text{Ag}_4(\mu\text{-dmpz})_8]$ also reflect to the changes in the average $\text{N}-\text{M}\cdots\text{M}-\text{N}$ torsion angles (**7**, 21.5°; $[\text{Pd}(\text{dmpz})_2(\text{dmpzH})_2]_2$, 21.8°; **5**, 8.3°; $[\text{Pd}_2\text{Ag}_4(\mu\text{-dmpz})_8]$, 6.0°). In both the Pt and Pd systems, two MN_4 coordination planes approach the eclipsed conformation by the replacement of the bridging hydrogen atoms with Ag^+ ions.

Summary

We have succeeded in obtaining the cyclic trinuclear Pd(II) complex $[\text{Pd}_3(\mu\text{-pz})_6]$ (**1**) with the simplest pyrazolate. The use of 4-methylpyrazole instead of pyrazole also afforded the trinuclear complex $[\text{Pd}_3(\mu\text{-4-Mepz})_6]$ (**2**). The most important factor for the preparation of cyclic trinuclear Pd(II) complex is the concentration of the reacting solution: the preparation in a dilute solution gives the trinuclear complex in higher yield. The absence of an appropriate base in the reaction afforded a mononuclear complex $[\text{Pd}(\text{pzH})_4]\text{Cl}_2$ (**6**). The reaction of $[\text{PtCl}_2(\text{C}_2\text{H}_5\text{CN})_2]$ with pzH in the presence of Et_3N afforded a known dimeric Pt(II) complex, $[\text{Pt}(\text{pz})_2(\text{pzH})_2]_2$ (**7**), even by refluxing in $\text{C}_2\text{H}_5\text{CN}$. Although the hydrogen-bonded dimer **7** requires a high temperature (185 °C) to form cyclic trimer $[\text{Pt}_3(\mu\text{-pz})_6]$ (**8**), *trans*- $[\text{PtCl}_2(\text{pzH})_2]$ without hydrogen bonding can be converted to **8** at a lower temperature (82 °C) under refluxing in CH_3CN . When the 3-*t*-BupzH, having a bulky substituent group at the 3-position on the pz ring, was employed, the reaction with $[\text{PdCl}_2(\text{CH}_3\text{CN})_2]$ afforded the neutral dinuclear complex $[\text{Pd}_2(\mu\text{-3-}t\text{-Bupz})_2(3\text{-}t\text{-Bupz})_2(3\text{-}t\text{-BupzH})_2]$ (**3**) with intramolecular hydrogen bonding. The removal of protons participating in the hydrogen bonding in **3** and **7** by Et_3N or Proton Sponge was not successful in CH_3CN that was not completely dried. These protons can be easily replaced by Ag^+ ions to give neutral heteronuclear complexes, $[\text{Pd}_2\text{Ag}_2(\mu\text{-3-}t\text{-Bupz})_6]$ (**4**) and $[\text{Pt}_2\text{Ag}_4(\mu\text{-pz})_8]$ (**5**), respectively.

Acknowledgment. This work was supported by a Grant-in-Aid for Scientific Research (No. 15550053) to K.U. We are grateful to the reviewers for valuable suggestions.

Supporting Information Available: Details of the check of the reaction conditions concerning the conversion of $[\text{Pt}(\text{pz})_2(\text{pzH})_2]_2$ to $[\text{Pt}_3(\mu\text{-pz})_6]$ and reaction of $[\text{PdCl}_2(\text{CH}_3\text{CN})_2]$ with KBpz_4 , crystal structures of $[\text{Pd}_3(\text{pz})_6]$, $[\text{Pd}_3(\text{pz})_6]\cdot 2\text{CH}_3\text{CN}$, and $[\text{Pd}(\text{pzH})_4]\text{Cl}_2\cdot\text{H}_2\text{O}$, X-ray crystallographic data in CIF format for the seven compounds in Table 1, and preliminary X-ray crystal data for $[\text{Pt}_3(\mu\text{-pz})_6]\cdot n\text{CH}_3\text{CN}$. This material is available free of charge via the Internet at <http://pubs.acs.org>.

IC026196G